

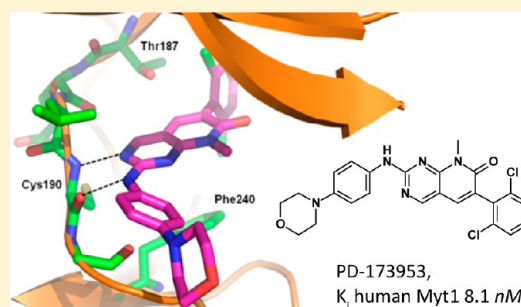
Application of Docking and QM/MM-GBSA Rescoring to Screen for Novel Myt1 Kinase Inhibitors

Kanin Wichapong,[†] Alexander Rohe,[†] Charlott Platzer,[†] Inna Slynko,[†] Frank Erdmann,[‡] Matthias Schmidt,[†] and Wolfgang Sippl^{*,†}

[†]Department of Pharmaceutical Chemistry and [‡]Department of Pharmacology, Martin-Luther-University Halle-Wittenberg, 06120, Halle (Saale), Germany

S Supporting Information

ABSTRACT: Identification of compounds that can bind to a target protein with high affinity is a nontrivial task in structure-based drug design. Several approaches ranging from simple scoring methods to more computationally demanding methods are usually applied for this purpose. In the current work, we used ligand docking in combination with QM/MM-GBSA, MM-GBSA, and MM-PBSA rescoring to discriminate between active and inactive Myt1 kinase inhibitors. Results show that QM/MM-GBSA rescoring performs better than normal docking scores or MM-GBSA rescoring in classifying active and inactive inhibitors. We also applied QM/MM-GBSA rescoring to estimate the binding affinities of compounds from different virtual screening runs. To prove our approach and to confirm its predictive power, a few compounds which were predicted to be active were purchased and experimentally tested. Among the five selected compounds, three showed significant inhibition of recombinant Myt1. PD-173952, which yielded a favorable QM/MM-GBSA binding free energy, showed a K_i value of 8.1 nM. In addition, two compounds, PD-180970 and saracatinib, showed inhibition at the low micromolar level. Thus, the developed protocol might be useful for further virtual screening experiments to better discriminate between active and inactive compounds and to further optimize the identified hits.



1. INTRODUCTION

A challenging task in drug discovery is to identify compounds that can bind to a specific target protein with high affinity and selectivity. Molecular docking represents a fast and simple computational method. Thus, this approach is frequently used for screening compounds from large databases. Simple scoring functions are, in addition, often applied to estimate the binding affinity of identified virtual screening hits. However, docking scores show often no correlation with experimental binding affinities^{1–3} and are not accurate enough to discriminate active from inactive compounds especially in the case where protein flexibility and solvation effects come into play. Therefore, more accurate methods such as binding free energy calculations are regularly employed for the postprocessing of docking results. This approach treats protein and ligand as flexible by carrying out energy minimization and/or molecular dynamics (MD) simulation. In addition, solvation effects can be considered by carrying out MD simulations using implicit (GBSA or PBSA model) or explicit solvent models.

In our previous work,⁴ we used binding free energy calculations to estimate the binding affinities of Wee1 kinase inhibitors using single protein–ligand complexes. We observed that using a single protein–inhibitor complex and MM-PBSA rescoring was sufficient to correctly rank the Wee1 inhibitors under study. Therefore, we became interested in applying the methodology to the related kinase Myt1. Myt1 kinase, which belongs to the same kinase family as Wee1, regulates the cell

cycle at G2/M transition.⁵ Many cancer cells lack a functional p53 signaling pathway, which means that the G1 checkpoint does not act as a control mechanism anymore. Thus the cancer cells rely on the G2 checkpoint more than the normal cells.^{6,7} Targeting proteins controlling the G2/M checkpoint is therefore another promising strategy for developing selective drugs for cancer therapy. We tested a diverse set of known kinase inhibitors for their inhibition of Myt1 kinase.⁸ Our screening results were in agreement with results published recently by Davis et al. who described the first three Myt1 kinase inhibitors (PD-173955, dasatinib, and SKI-606).⁹ Interestingly, only a few compounds exhibited activities against Myt1 kinase; whereas, most of the known kinase inhibitors, even very promiscuous ones such as staurosporine, PKC-412, bisindolyl-maleimide I, and sunitinib, did not reveal any inhibition or binding.⁸

MM-PBSA and MM-GBSA methods (molecular mechanic Poisson–Boltzmann surface area and molecular mechanic generalized Born surface area) are widely used for estimating the binding free energy of protein–ligand complexes derived from docking calculations. Several studies^{10–12} have demonstrated that the binding affinities of inhibitors can be approximated by calculating the binding free energy using the MM-PBSA or MM-GBSA methods. The time requirement for

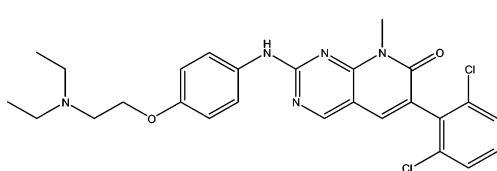
Received: December 10, 2013

Published: February 3, 2014

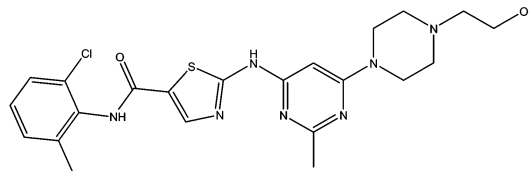
computing the binding free energy using this approach can be reduced by using a single complex obtained by energy minimization^{2,4,13,14} instead of using an ensemble derived from MD simulations. Thus, we applied these methods for rescoring compound identified by virtual screening of different compound libraries.

2. COMPUTATIONAL METHODS AND EXPERIMENTAL SECTION

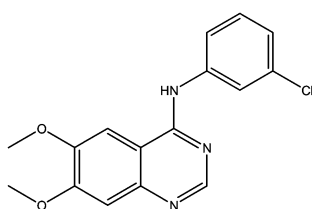
2.1. Ligand Preparation and Molecular Docking. All ligands were built using MOE2011.10¹⁵ and optimized using the MMFF94 force field with a convergence criteria of 0.01 kcal/mol. The protonate-3D module in MOE2011.10 was used to



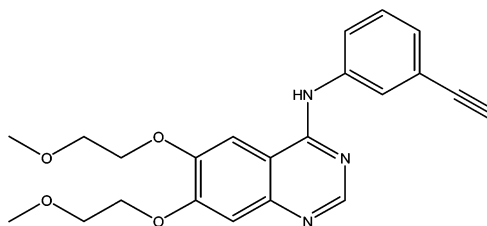
PD-0166285



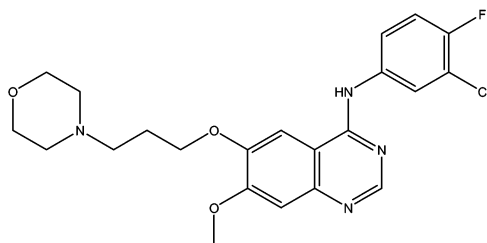
Dasatinib



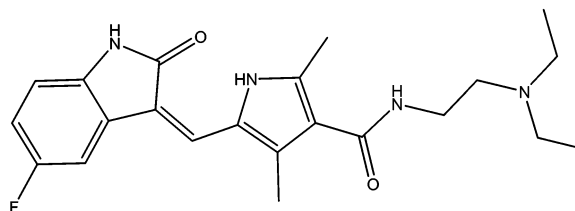
Tyrphostin AG 1478



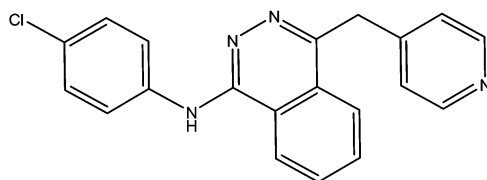
Erlotinib



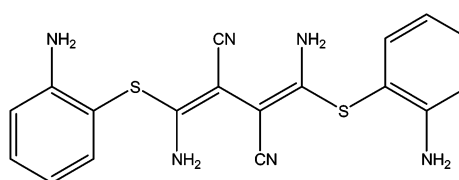
Gefitinib



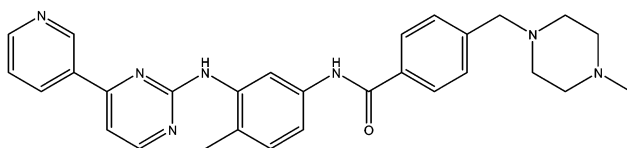
Sunitinib



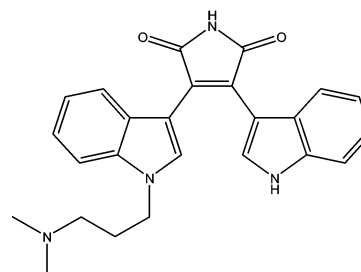
Vatalanib



U0126



Imatinib



Bisindolyl-maleimide I

Figure 1. continued

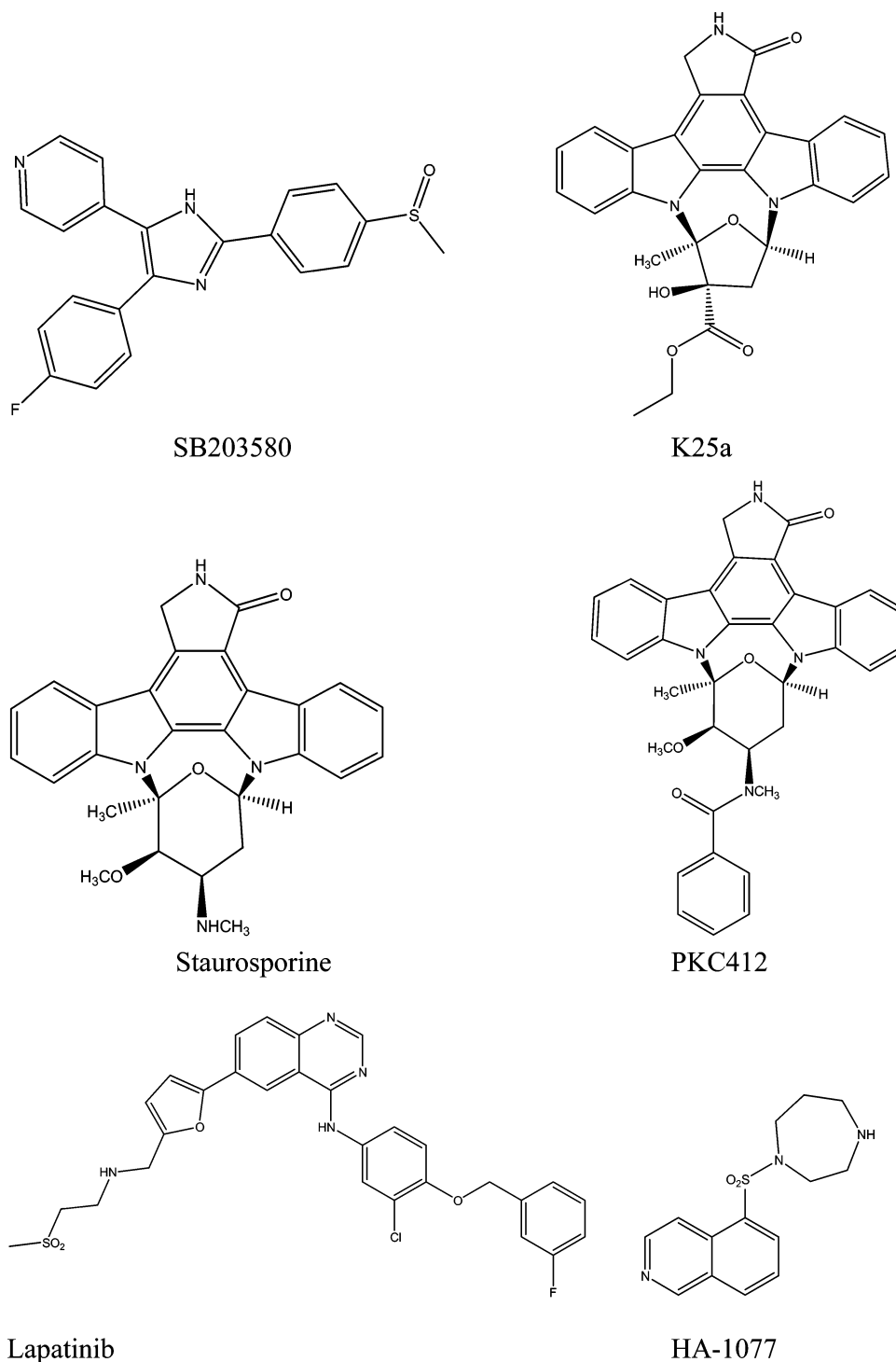


Figure 1. Structures of compounds, which were tested in vitro against Myt1 kinase. Biological data are given in Table 1

determine the protonation state of these compounds at pH 7.1. Molecular docking of the ligands into the binding pocket of Myt1 kinase (PDB code 3P1A) was performed using the docking program GOLD version 5.0.^{16,17} The potential binding pocket was defined using Cys190 as a center and a radius of 20 Å. Twenty docking solutions were calculated for each compound. Water molecules located at the binding pocket of Myt1 kinase were considered for docking using the “toggle” mode in GOLD.

2.2. Binding Free Energy Calculation. Binding free energy methods (MM-PB(GB)SA and QM/MM-GBSA) were applied to estimate the binding affinities of the compounds under study.

As previously reported,^{4,13,18,19} the conformation of the complex derived from energy minimization was considered for calculating the binding free energy. Before performing energy minimization, force field and charges for ligand and protein were first assigned using the LEaP module in AMBER11,²⁰ general amber force field (GAFF)²¹ with AM1-BCC charge²² for the ligand, and the Amber03 force field for the protein. Then, all docking solutions were energy minimized using 2000 steps of steepest descent and followed by 2000 steps of conjugate gradient algorithm in continuum solvent (GB model)^{23,24} in AMBER11. The energy minimized complexes were subsequently applied to calculate the

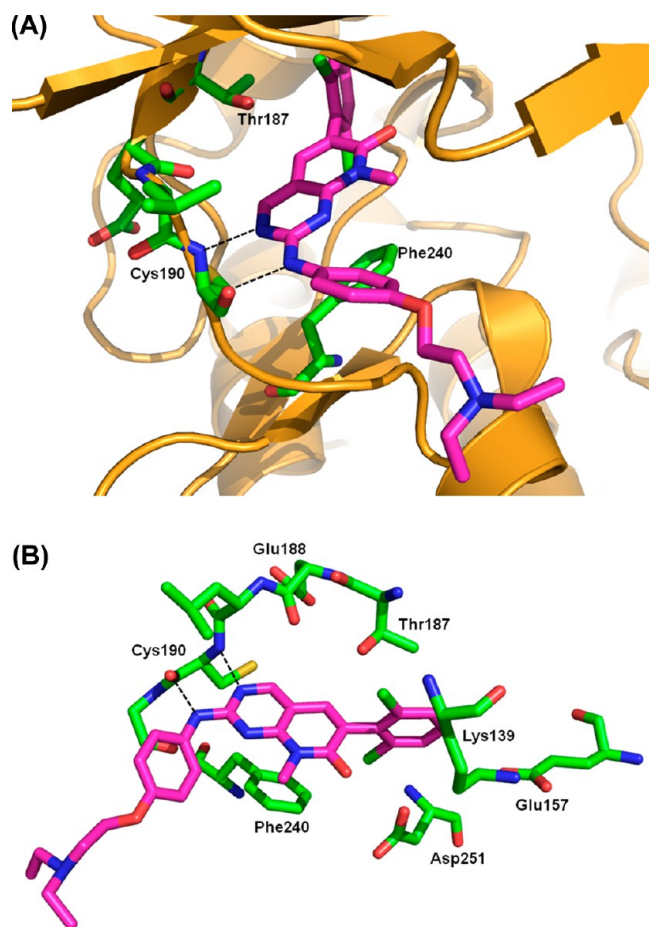


Figure 2. (A) Predicted binding mode of the active compound (PD-1066285, colored magenta). The Myt1 kinase is shown as orange ribbon and green sticks. H-bond interactions are displayed as dashed lines. (B) Closer look to the hydrophobic pocket near the gatekeeper Thr187. Interacting amino acid residues are shown as green sticks.

binding free energy using the MM-PB(GB)SA module implemented in AMBER11. The binding free energy was computed based on the equations shown below:

$$\Delta G_{\text{binding}} = G_{\text{complex}} - G_{\text{protein}} - G_{\text{ligand}} \quad (1)$$

$$G = H - T\Delta S \quad (2)$$

and

$$H = E_{\text{vdW}} + E_{\text{ele}} + E_{\text{int}} + G_{\text{sol}} \quad (3)$$

where H and $-T\Delta S$ are the enthalpy and entropy change upon ligand binding. E_{vdW} , E_{ele} , and E_{int} represent van der Waals, electrostatic interaction, and internal energy, respectively. G_{sol} is the free energy of solvation which was calculated by solving GB^{23,24} or PB²⁵ model.

Binding free energy using QM/MM-GBSA method was also computed by using QM/MM-GBSA module in AMBER11. The same equations (eqs 1–3) as MM-PB(GB)SA was used, but the enthalpy terms were computed by applying the QM/MM approach. The free energy of solvation was calculated using the GB model. The QM region was defined by 5 Å around the binding pocket, including ligand and residues from the hinge region, the P-loop, the hydrophobic pocket, and DFG motif. The QM region was set the same for every system, and two QM methods (RM1 and AM1) were examined. As previously

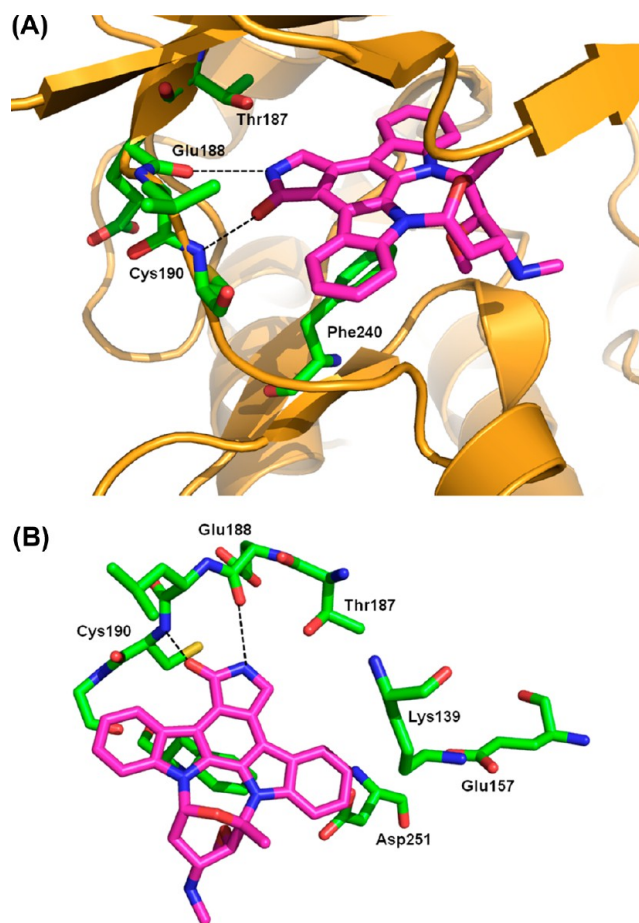


Figure 3. (A) Predicted binding mode of the inactive compound staurosporine (colored magenta). The Myt1 kinase is shown as orange ribbon and green sticks. H-bond interactions are displayed as dashed lines. (B) Closer look to the hydrophobic pocket near the gatekeeper Thr187. Interacting amino acid residues are shown as green sticks.

reported, there is a correlation between the number of rotatable bonds of a ligand and the respective entropy values.²⁶ In addition, including the entropy value approximated from the number of rotatable bonds of the ligands into the binding free energy scoring can increase the correlation with the experimental data^{26,27} or improve the performance of virtual screening.²⁸ Thus, the entropy term was simply approximated from the number of rotatable bonds of the ligands (1.0 kcal/mol for one rotatable bond). The entropy values were summed together with the enthalpy derived from QM/MM-GBSA calculation, and thus, this value was called the QM/MM-GBSA score.

2.3. Molecular Dynamics (MD) Simulation. The complexes between Myt1 and active as well as inactive compounds were additionally subjected to MD simulations. The docking solutions of these compounds which were selected for binding free energy calculation were further subjected to structure refinement by performing MD simulations. The complexes were prepared using the same parameters as for energy minimization (Amber03 force field for protein and GAFF force field together with AM1-BCC charges for ligands). Waters (TIP3P model)²⁹ were added in the radius within 10 Å from the molecular surface of the complex. In order to neutralize the system some waters were replaced by counterions (Na^+ or Cl^-). To relax the system prior to performing MD simulations, two consecutive steps of energy minimization were employed; 2000 steps minimization

only of the solvent and followed by 5000 steps minimization of the whole system. After that, the system was slowly heated up from 0 to 300 K during the first few picoseconds and kept constant at this temperature by applying Langevin dynamics³⁰ with a collision frequency of 1 ps⁻¹. The position-restrained phase of MD simulation was run through the first 100 ps of the simulation by restraining the position of the complex with a weak force constraint (10 kcal/mol) and also constraining the volume. Finally, free MD simulations were employed from 100 ps to 10 ns using NPT ensemble (a constant pressure at 1 bar and the constant temperature at 300K). A time step of 2 fs with SHAKE algorithm³¹ was applied to keep all bonds involving hydrogen atoms rigid. The particle-mesh-Ewald (PME)³² method was used for calculating electrostatic interaction, and the cutoff of nonbonded interaction was set to 10 Å.

2.4. Myt1 Kinase Expression and Purification. All steps were carried out as described by Rohe et al.³³ Briefly, the human Myt1 75-362 fragment was cloned into the pET28 vector and the final construct was transformed into *E. coli* BL21(DE3). Bacteria were grown at 37 °C until the OD600 reached 0.6, and then the temperature was adjusted to 22 °C. Expression of kinase fragment was induced by addition of IPTG at OD600 = 1.0. Cells were harvested by centrifugation, and the pellet was resuspended in binding buffer and frozen at -20 °C. Thawed bacterial cells were disrupted by sonication on ice. After centrifugation, the supernatant containing the Myt1 75-362 fragment as His₆-tagged protein was applied on 1 mL Ni²⁺-NTA HiTrap column (GE Healthcare), and all following purification steps were performed according to the manufacturer's instructions.

2.5. Myt1 Binding Assay. A fluorescence anisotropy based kinase binding assay procedure as described recently³⁴ was applied to test the biological activities of the compounds selected by the described method. A fluorescently labeled kinase tracer based on dasatinib binds to the kinase, yielding a high anisotropy value. While a nonbinder does not affect this equilibrium, a binder displaces the tracer from the kinase, leading to a decreased fluorescence anisotropy. Emission intensities were measured in two perpendicular channels at 485 nm (ex)/520 nm (em). For improved comparability among experiments, anisotropy values were normalized against positive controls (10 μM Dasatinib) and negative controls (vehicle, 1% DMSO) and reported as [% tracer displaced]. Assays were performed in sterile-filtered kinase buffer (50 mM HEPES pH 7.5, 0.03% CHAPS, 10 mM MgCl₂, and 1 mM DTT) in black 96-well half a rea plates (Corning). Compounds were purchased from Key Organics (Camelford, UK) and LC Laboratories (Woburn, MA, US) and tested at a concentration of 10 and 20 μM in three independent experiments. Compounds exhibiting significant displacement at the indicated concentrations were carried on to further IC₅₀ value determinations and subsequent K_i calculations. In this assay, the positive controls PD-0166285 and dasatinib had an IC₅₀ value of 31.1 nM (K_i = 2.0 nM) and 201.7 nM (K_i = 73 nM), respectively, which is in agreement with published data.^{8,9}

3. RESULTS AND DISCUSSION

3.1. Docking and Scoring of Myt1 Kinase Inhibitors. We started with docking the kinase inhibitors recently tested in our laboratory⁸ (chemical structures of these inhibitors shown in Figure 1). The used data set comprised five actives and eleven inactive compounds. Docking results of the active compounds (e.g., PD-0166285) and the inactive compounds (e.g., staurosporine) as displayed in Figures 2 and 3 showed a similar binding mode. The compounds form H-bonds with the

Table 1. GoldScores and Binding Free Energies Derived from MM-PBSA and MM-GBSA Calculations Using Single Protein–Ligand Complexes

cpd name	displacement [%] at 10 μ M ⁸	IC ₅₀ (nM) ⁸	GoldScore	binding free energy calculation						including entropy		
				ELE	VDW	GAS	G _{sol} PB	MM-PBSA	G _{sol} GB	MM-GBSA	MM-PBSA	MM-GBSA
PD0166285	Set to 100	7.2 ± 1.1	51.3	-56.78	-68.21	-124.99	87.72	-37.27	65.66	-59.33	-46.27	-68.33
dasatinib	97.1 ± 0.3	63.0 ± 1.1	51.9	13.02	-66.52	-53.50	19.38	-34.12	-8.03	-61.52	-42.12	-69.52
tyrphostin AG 1478	39.5 ± 1.5		47.5	-22.28	-52.65	-74.93	46.76	-28.17	32.03	-42.90	-32.17	-46.90
erlotinib	8.15 ± 0.65		44.1	-24.60	-64.49	-89.12	56.04	-33.08	38.28	-50.84	-44.08	-61.84
gefitinib	6.85 ± 2.35		50.9	-26.77	-65.18	-91.95	61.10	-30.85	37.57	-54.38	-38.85	-62.38
sunitinib	nd ^a		35.5	-25.87	-50.13	-76.00	39.41	-36.59	32.39	-43.61	-44.59	-51.61
vatalanib	nd		45.8	-17.75	-50.61	-68.36	48.21	-20.16	27.61	-40.75	-24.16	-44.75
U0126	nd		64.6	-49.42	-55.99	-105.41	66.78	-38.63	48.55	-56.86	-45.63	-63.86
imatinib	nd		43.1	-21.88	-57.67	-79.56	64.13	-15.42	38.31	-41.25	-23.42	-49.25
bisindolyl-maleimide I	nd		41.5	-42.97	-54.82	-97.79	62.44	-35.35	48.21	-49.58	-41.35	-55.58
SB203580	nd		58.4	-31.44	-46.23	-77.67	62.92	-14.75	47.07	-30.60	-18.75	-34.60
K252a	nd		59.8	-19.42	-60.21	-79.63	52.74	-26.89	36.63	-43.00	-28.89	-45.00
staurosporine	nd		54.0	-21.20	-57.98	-79.21	56.80	-22.41	37.48	-41.73	-24.41	-43.73
lapatinib	nd		47.9	-4.44	-63.61	-68.06	47.62	-20.44	28.54	-39.52	-31.44	-50.52
PKC412	nd		30.8	20.20	-72.93	-93.41	68.21	-25.20	42.81	-50.60	-29.20	-54.60
HA-1077	nd		35.8	-24.92	-44.01	-68.93	44.28	-24.65	30.72	-38.20	-26.65	-40.20

^aNo displacement at 10 μM.

Table 2. QM/MM-GBSA Score (Single Protein–Ligand Complexes) Obtained by Using Different QM Methods

cpd name	displacement [%] at 10 μM ⁸	IC ₅₀ (nM) ⁸	vdW	GAS	ESCF	GB _{solv}	num of rotatable bonds	QM/MM-GBSA score
QM method = RM1								
PD0166285	set to 100	7.2 \pm 1.1	−24.01	−24.01	−19.36	40.07	9	−12.30
erlotinib	8.15 \pm 0.65		−21.32	−21.33	−13.10	38.53	11	−6.91
gefitinib	6.85 \pm 2.35		−22.66	−22.65	−25.98	50.61	8	−6.03
tyrphostin AG 17478	39.5 \pm 1.5		−19.04	−19.04	−18.23	36.37	4	−4.90
dasatinib	97.1 \pm 0.3	63.0 \pm 1.1	−23.51	−23.49	45.51	−18.19	8	−4.17
sunitinib	nd ^a		−13.23	−13.22	−7.52	28.97	8	0.24
vatalanib	nd		−14.41	−14.41	−13.17	32.97	4	1.39
U0126	nd		−20.25	−20.26	−8.87	37.78	7	1.64
imatinib	nd		−15.85	−15.85	4.98	25.43	8	6.56
bisindolyl-maleimide I	nd		−20.11	−20.12	−27.30	64.49	6	11.06
SB203580	nd		−14.60	−14.61	−42.60	75.60	4	14.39
K252a	nd		−16.50	−16.50	−8.76	42.01	2	14.75
staurosporine	nd		−16.47	−16.47	−14.28	50.02	2	17.27
lapatinib	nd		−16.90	−16.91	2.33	43.49	11	17.90
PKC412	nd		−19.55	−19.56	−13.85	59.88	4	22.46
HA-1077	nd		−14.37	−14.38	−38.23	80.90	2	26.29
QM method = AM1								
PD0166285	set to 100	7.2 \pm 1.1	−24.01	−24.01	−14.57	42.33	9	−5.25
dasatinib	97.1 \pm 0.3	63.0 \pm 1.1	−23.51	−23.49	46.40	−16.68	8	−1.77
gefitinib	6.85 \pm 2.35		−22.66	−22.65	−21.80	51.02	8	−1.42
erlotinib	8.15 \pm 0.65		−21.32	−21.33	−11.67	43.58	11	−0.41
sunitinib	nd		−13.23	−13.22	−11.22	32.24	8	−0.21
tyrphostin AG 1478	39.5 \pm 1.5		−19.04	−19.04	−14.72	38.38	4	0.61
imatinib	nd		−15.85	−15.85	2.21	29.25	8	7.61
vatalanib	nd		−14.41	−14.41	−5.68	32.70	4	8.62
U0126	nd		−20.25	−20.26	−6.20	46.98	7	13.52
SB203580	nd		−14.60	−14.61	−39.09	74.86	4	17.16
staurosporine	nd		−16.47	−16.47	−22.05	60.62	2	20.10
K252a	nd		−16.50	−16.50	−12.70	51.63	2	20.43
bisindolyl-maleimide I	nd		−20.11	−20.12	−28.25	75.34	6	20.98
lapatinib	nd		−16.90	−16.91	9.94	41.14	11	23.16
PKC412	nd		−19.55	−19.56	−22.17	71.07	4	25.35
HA-1077	nd		−14.37	−14.38	−32.03	74.02	2	25.62

^aNo displacement at 10 μM .

Table 3. Binding Free Energies (MM-PBSA and MM-GBSA) Calculated by Using Average Snapshots from MD Simulation

cpd name	displacement [%] at 10 μM ⁸	IC ₅₀ (nM) ⁸	vdW	ELE	GAS	G _{sol} (PB)	MM-GBSA	G _{sol} (GB)	MM-PBSA	num of rot bonds	MM-GBSA (include entropy)	MM-PBSA (include entropy)
PD0166285	set to 100	7.2 \pm 1.1	−54.70	−45.57	−100.27	50.63	−49.64	64.23	−36.04	9	−58.64	−45.04
dasatinib	97.1 \pm 0.3	63.0 \pm 1.1	−57.74	−9.97	−67.71	12.94	−54.77	29.21	−38.50	8	−62.77	−46.5
tyrphostin AG 1478	39.5 \pm 1.5		−43.97	−10.14	−54.11	20.69	−33.42	30.34	−23.77	4	−37.42	−27.77
erlotinib	8.15 \pm 0.65		−55.14	−24.28	−79.42	36.65	−42.77	50.39	−29.03	11	−53.77	−40.03
gefitinib	6.85 \pm 2.35		−57.15	−17.17	−74.31	30.02	−44.29	43.21	−31.11	8	−52.29	−39.11
bisindolyl-maleimide I	nd ^a		−47.45	−40.01	−87.46	46.68	−40.78	56.30	−31.16	6	−46.78	−37.16
imatinib	nd		−53.75	−85.03	−138.78	93.56	−45.22	106.62	−32.16	8	−53.22	−40.16
staurosporine	nd		−56.25	−34.82	−91.07	42.58	−48.49	56.12	−34.95	2	−50.49	−36.95

^aNo displacement at 10 μM .

backbone of Cys190 located at the hinge region. The binding mode of staurosporine exhibited an additional H-bond interaction with Glu188. Also the other kinase inhibitors showed a very similar binding mode including hydrogen bonds with residues of the hinge region (Glu188 and Cys190). Docking scores obtained for active and inactive compounds were found to be similar (e.g GoldScore) as listed in Table 1. For instance,

dasatinib and PD-0166285 (actives) yielded GoldScores of 51.9 and 51.3, while inactives such as K252a or U0126 produced even higher GoldScores (59.8 and 64.6, respectively). These results indicate that the docking scores are not able to discriminate between active and inactive compounds. Other scoring functions implemented in GOLD were tested (ChemScore, PLP, ASP) and showed similarly discouraging results.

Table 4. QM/MM-GBSA Energies Obtained by Using Average Snapshots from MD Simulation Compared to Using a Single Complex Derived by Energy Minimization

compound	displacement [%] at 10 μ M ⁸	IC ₅₀ (nM) ⁸	prediction	vdW	GAS	ESCF	GB _{solv}	num of rot bonds	QM/MM-GBSA score (MD)	QM/MM-GBSA score (single complex)
PD0166285	set to 100	7.2 \pm 1.1	highly active	−17.52	−17.50	−23.11	40.78	9	−8.83	−12.30
dasatinib	97.1 \pm 0.3	63.0 \pm 1.1	active	−19.13	−19.10	10.85	12.25	8	−4.01	−4.17
tyrphostin AG 1478	39.5 \pm 1.5		weakly active	−14.71	−14.61	−8.29	24.23	4	−2.67	−4.90
erlotinib	8.15 \pm 0.65		weakly active	−18.12	−18.06	−12.90	35.58	11	−6.38	−6.91
gefitinib	6.85 \pm 2.35		weakly active	−18.79	−18.90	−11.18	36.12	8	−1.95	−6.03
bisindolyl-maleimide I	nd ^a		inactive	−16.64	−16.64	−25.82	52.16	6	3.70	11.06
imatinib	nd		inactive	−11.14	−11.08	−84.37	108.75	8	5.30	6.56
staurosporine	nd		inactive	−17.18	−17.32	−27.89	51.02	2	3.81	17.27

^aNo displacement at 10 μ M.Table 5. QM/MM-GBSA Score (Single Protein–Ligand Complex) Obtained by Using Different Myt1 Conformations Including the X-ray Structure and Snapshots Derived from Different MD Runs^a

compound	displacement [%] at 10 μ M ⁸	IC ₅₀ (nM) ⁸	Myt1 X-ray structure		Myt–PD01662865 complex MD		Myt–staurosporine complex MD		free-ligand Myt1MD	
			scoring-based pose	energy-minimized pose	scoring-based pose	energy-minimized pose	scoring-based pose	energy-minimized pose	scoring-based pose	energy-minimized pose
PD0166285	set to 100	7.2 \pm 1.1	49.30	−12.30	27.31	−18.35	46.60	−3.25	46.09	−9.07
erlotinib	8.15 \pm 0.65		16.43	−6.91	14.77	−10.02	14.87	−8.17	53.26	−3.53
gefitinib	6.85 \pm 2.35		18.43	−6.03	22.37	−5.08	78.65	−3.71	76.13	−2.26
tyrphostin AG 1478	39.5 \pm 1.5		33.94	−4.90	21.84	−2.02	25.81	−10.16	44.62	−1.45
dasatinib	97.1 \pm 0.3	63.0 \pm 1.1	52.17	−4.17	26.38	−3.29	c	c	62.30	9.39
sunitinib	nd ^b		63.47	0.24	c	c	c	c	46.50	−5.68
vatalanib	nd		55.34	1.39	17.84	2.46	19.91	−6.05	38.88	1.68
U0126	nd		49.71	1.64	65.72	−0.89	18.19	−5.79	129.35	7.68
imatinib	nd		67.13	6.56	94.17	21.30	99.14	22.83	152.77	28.62
bisindolyl-maleimide I	nd		86.79	11.06	95.39	3.60	33.63	−0.59	187.46	13.17
SB203580	nd		35.68	14.39	82.03	22.60	43.48	31.18	74.93	16.38
K252a	nd		34.72	14.75	131.30	20.48	c	c	c	c
staurosporine	nd		110.16	17.27	c	c	26.63	2.23	c	c
lapatinib	nd		90.59	17.90	65.24	7.97	73.38	20.66	173.61	6.67
PKC412	nd		76.83	22.46	c	c	23.29	5.23	c	c
HA-1077	nd		95.19	26.29	55.63	27.75	57.54	21.76	113.32	33.92

^aFor each ligand, the scoring-based pose (without energy minimization) and energy-minimized pose was used for the calculation. All QM/MM-GBSA scores are given in kilocalories per mole. ^bNo displacement at 10 μ M. ^cNo favorable binding mode observed.

3.2. Binding Free Energy Calculations. We rescored the derived docking poses by calculating the binding free energy applying the MM-PBSA and MM-GBSA methods. The top-ranked pose from MM-PBSA rescoring was selected. Some of the studied inhibitors have already been cocrystallized with other kinases. For these inhibitors, the top-ranked binding pose from MM-PBSA was compared with the cocrystal structures. Results illustrated that the top-ranked MM-PBSA pose showed the same binding mode known from other kinase X-ray structures (e.g., dasatinib as shown in Supporting Information Figure S1). However, the calculated MM-PBSA or MM-GBSA energies were also not able to discriminate active from inactive compounds as shown in Table 1. For example, MM-PBSA values of the highly active compounds, PD-0166285 and dasatinib, were −37.27 and −34.12 kcal/mol, respectively. For the inactive compounds similar values were obtained, e.g. sunitinib −36.59 kcal/mol,

U0126 −38.63 kcal/mol, or bisindolyl-maleimide I −35.35 kcal/mol. Similar findings were observed using the MM-GBSA approach (see Table 1). The obtained results imply that MM-PBSA and MM-GBSA values derived from single protein–ligand complexes are not accurate enough to discriminate between active and inactive Myt1 kinase inhibitors.

In a next step, we tested the QM/MM-GBSA rescoring method. The results of the QM/MM-GBSA rescoring are summarized in Table 2. By using the semiempirical RM1 method PD-0166285, erlotinib, gefitinib, tyrphostin AG 1478, and dasatinib gave favorable values indicating that the method is able to correctly identify the compounds binding to Myt1. The inactive compounds yielded positive values implying an unfavorable binding to Myt1 kinase. The QM/MM-GBSA scores of the active compounds (−4 to −12 kcal/mol) are obviously different from those of the inactive compounds (0 to 26 kcal/mol). In case of AM1, similar

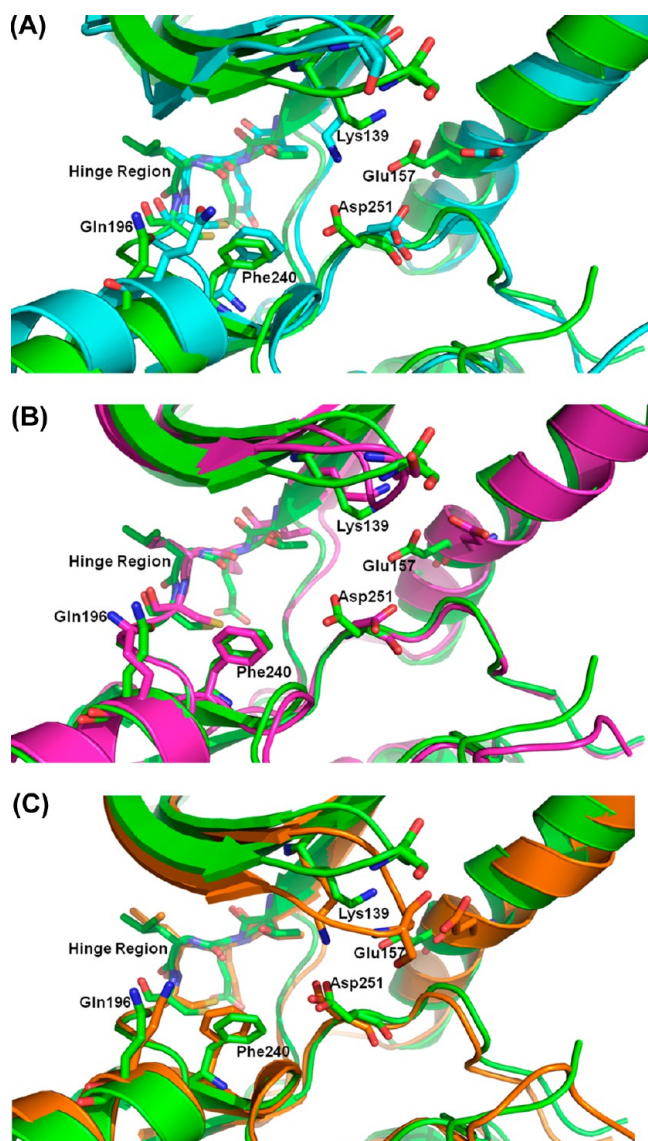


Figure 4. (A) Comparison of the Myt1 X-ray structure (PDB Code 3P1A, green ribbon and sticks) and a Myt1 conformation derived from the last snapshot of the MD simulation of Myt1 in complex with PD01662865 (cyan ribbon and sticks). A RMSD value of 2.80 Å is observed. (B) Comparison of the Myt1 X-ray structure (green ribbon and sticks) and a Myt1 conformation obtained from the last snapshot of the MD simulation of Myt1 in complex with staurosporine (magenta ribbon and sticks, RMSD = 1.45 Å). (C) Comparison of the Myt1 X-ray structure (green ribbon and sticks) and a Myt1 conformation retrieved from the last snapshot of the MD simulation of free Myt1 (orange ribbon and sticks, RMSD = 2.08 Å).

results were obtained. Most of the active compounds gave negative QM/MM-GBSA scores except tyrphostin AG 1478 (0.61 kcal/mol). Only one inactive compound was wrongly predicted by using the AM1 method, which is sunitinib that showed a negative QM/MM-GBSA score (−0.21 kcal/mol). Again, it can be seen that the QM/MM-GBSA scores of the active compounds (0.6 to −5 kcal/mol) noticeably differ from the ones of the inactive compounds (7 to 25 kcal/mol) when excluding sunitinib. In conclusion, the QM/MM-GBSA scores perform very well to discriminate between active and inactive Myt1 inhibitors. As RM1 performed better than AM1, henceforth semiempirical RM1 method was applied to calculate QM/MM-GBSA scores.

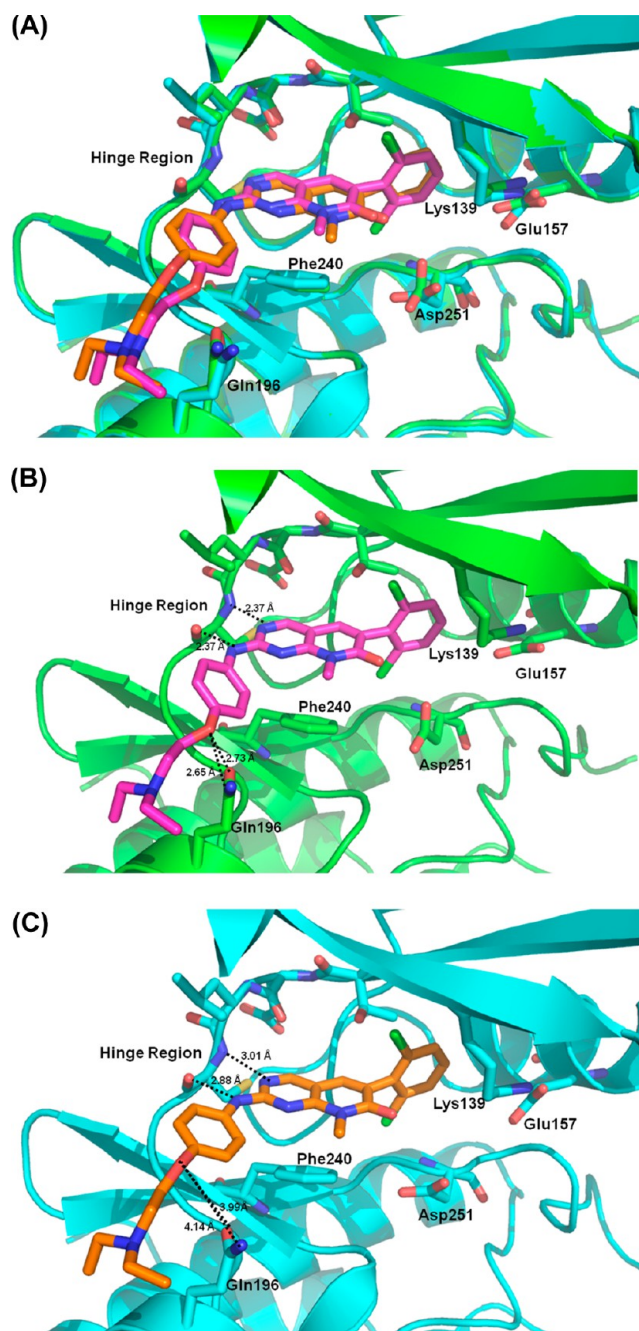
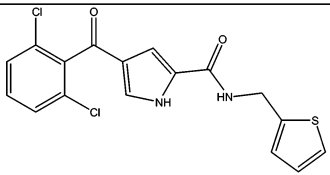
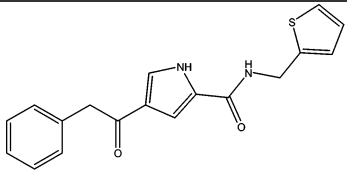
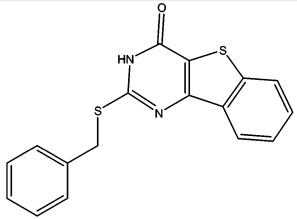
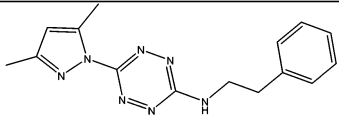
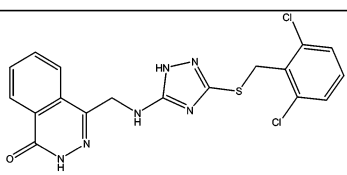
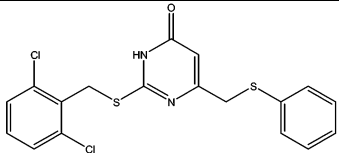
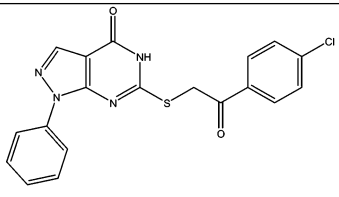


Figure 5. (A) Comparison of the conformation of PD01662865 and interacting residues at the binding pocket before energy minimization (Myt1 colored green and PD01662865 colored magenta) and after energy minimization (Myt1 colored cyan and PD01662865 colored orange). (B) Docking pose of PD01662865 derived using the Myt1 X-ray structure. The distance of close contact between Myt1 (green sticks) and PD01662865 (magenta sticks) is indicated. (C) Close contacts could be removed by applying an energy minimization protocol (cyan = Myt1 and orange = PD01662865).

3.3. Binding Free Energies Derived from MD Simulation. Next, we tested whether sampling of the conformational space of protein–inhibitor complexes is more suitable for predicting the binding free energies. For this purpose, we carried out MD simulations for 10 ns for some selected protein–inhibitor complexes. The six active inhibitors (PD-0166285, dasatinib, tyrphostin AG 178, erlotinib, and gefitinib) and three structurally diverse inactive compounds (imatinib, bisindolyl-maleimide I,

Table 6. Chemical Structure, Predicted, and Experimental Myt1 Kinase Inhibition of Key Organic Compounds^a

Compound	Chemical structure	QM/MM-GBSA energy (kcal/mol)	Prediction	Myt1 in vitro results (Ki)
1R-0035		1.46	Inactive	n.e.
1R-0046		7.56	Inactive	n.e.
2R-1301		14.48	Inactive	n.e.
7G-003		3.90	Inactive	n.e.
8D-022		3.70	Inactive	n.e.
9L-564S		3.73	Inactive	n.e.
9N-661S		2.90	Inactive	n.e.

^an.e. = no effect.

and staurosporine) were selected. For each compound 20 snapshots from the last 3 ns of the simulations were extracted for calculating the binding free energy applying the MM-PB(GB)SA and QM/MM-GBSA methods. The root-mean-square deviation (RMSD) of the protein and the inhibitors (Supporting Information Figure S2) showed small fluctuations indicating the stability of these complexes during the simulation. The MM-PB(GB)SA values derived from the selected snapshots (summarized in Table 3) showed again that the values for active and inactive compounds are roughly in the same range (MM-GBSA actives -33.42 to -54.77 kcal/mol, inactives

-40.78 to -48.49 kcal/mol; MM-PBSA actives -23.77 to -38.50 kcal/mol, inactives -31.16 to -34.95 kcal/mol), even though the entropy values approximated from the number of rotatable bonds of ligand were included (Table 3). Thus, these results confirmed that MM-PB(GB)SA either obtained from a single complex or an ensemble from MD simulations cannot be used to classify active or inactive Myt1 kinase inhibitors.

Next, we calculated the QM/MM-GBSA energies for the snapshots derived from the MD simulations (Table 4). The calculated energies can be used to discriminate between active and inactive inhibitors. The values of the active compounds were

found to be negative (−1.95 to −8.83 kcal/mol); whereas the inactives show positive values (3.70 to 3.81 kcal/mol). The QM/MM-GBSA energies obtained from using MD snapshots are also able to separate highly active from moderately or weakly active compounds. The QM/MM-GBSA energies derived from the MD simulation are able to correctly rank the inhibitors: PD-1066285 > erlotinib > dasatinib > tyrphostin AG 1478 > gefitinib which is very similar to the experimental data (Table 4).

3.4. Influence of Myt1 Conformations for Molecular Docking and Binding Free Energy Calculation. Finally, we investigated the influence of the protein conformation used for docking and binding free energy calculations. The X-ray structure of Myt1 kinase and several Myt1 conformations derived from MD runs (Myt1-PD01066285 complex, Myt1-staurosporine complex, and free-ligand Myt1) were selected for this purpose. The MD simulations were carried out for 10 ns and the last snapshot of the MD simulation was selected for docking and binding free energy calculations. In general, the conformation of these complexes is quite similar (RMSD values between 1.45 and 2.80 Å), except some residues located in the binding pocket (i.e., Lys139, Glu157, Gln196, Phe240, and Asp251) that showed different conformations (Figure 4). However, we found that using Myt1 conformations derived from MD snapshots for docking calculation can result in producing wrong binding mode for some compounds (some examples are shown in Figure S3 in the Supporting Information). On the other hand, all compounds can be docked into the X-ray structure of Myt1 (Figures 2, 3, and S1). Moreover, we also compared the binding free energies calculated for the scoring-based poses (without energy minimization) and optimized poses (with energy minimization). Binding free energies of the scoring-based poses either derived by using the X-ray structure or MD snapshots were found to be relatively high (more positive values as summarized in Table 5). This can be due to some close contacts between atoms generated by docking calculations as shown in Figure 5A and B. A short energy minimization as applied in the current study allows the ligand to better fit in the binding pocket and can remove all of these close contacts as demonstrated in Figure 5C. As a consequence, the binding free energies of energy-minimized poses are significantly lower and more favorable. Using protein structures derived from MD simulations did not improve binding free energy calculation, and no discrimination between active and inactive compounds was observed (Table 5).

In conclusion, the X-ray structure of Myt1 represents the most suitable Myt1 conformation for docking and binding free energy calculations. A short energy minimization is required and sufficient to optimize the docking poses. Thus, the Myt1 X-ray structure and the energy minimization together with the binding free energy protocol (QM/MM-GBSA score) are further applied in order to identify novel Myt1 kinase inhibitors.

3.5. Evaluating the Predictivity of the QM/MM-GBSA Rescoring Method. Next, we tested the performance of the QM/MM-GBSA rescoring on further compounds that we recently tested in vitro. In some previous work, seven compounds from the Keyorganics compound collection were chosen on the basis of GOLD docking results, and were found to be inactive in the in vitro assay (Table 6). As the binding mode of the Keyorganic compounds is not known, we selected the docking poses based on the calculated MM-PBSA and MM-GBSA scores. All compounds showed at least one hydrogen bond to the hinge region residues and favorable GoldScores (data not shown). The selected docking solutions were then used to calculate the binding free energy applying the QM/MM-GBSA rescoring and

using minimized protein–inhibitor complexes. As summarized in Table 6, the QM/MM-GBSA scores of all seven compounds gave positive QM/MM-GBSA scores implying that these compounds are inactive, which is in agreement with the in vitro testing.

Since it turned out so far, that it is difficult to identify novel potent Myt1 inhibitors,^{8,9} we selected 23 known kinase inhibitors from the literature and predicted the binding free energy applying the QM/MM-GBSA rescoring approach. The binding mode of these compounds for kinases is in most cases known. Thus, we selected the GOLD docking pose that was similar to the binding mode observed for other kinases. The predicted binding free energies using energy-minimized kinase–inhibitor complexes and the QM/MM-GBSA rescoring approach of the 23 compounds are summarized in Table 7. Four compounds

Table 7. Predicted and Experimental Myt1 Kinase Inhibition of Tested Kinase Inhibitors

compound	QM/MM-GBSA energy (kcal/mol)	prediction	Myt1 in vitro results (K_i)
PD-173952	−5.99	active	8.1 ± 3.6 nM
PD-180970	−5.85	active	1.35 ± 0.27 μ M
CUDC-101	−8.02	active	ne ^a
saracatinib	−6.24	active	5.2 ± 1.5 μ M
tivozanib	−4.92	weakly active	ne
tyrphostin 48	0.61	inactive	nt ^b
GDC-0941	26.44	inactive	nt
KU-0063794	6.16	inactive	nt
PIK-90	0.33	inactive	nt
CHIR911	4.60	inactive	nt
PD 98059	0.37	inactive	nt
Mubritinib	2.26	inactive	nt
Go 6976	14.25	inactive	nt
H-89	23.55	inactive	nt
LY 294002	2.26	inactive	nt
MK1775	4.57	inactive	nt
OSU-03012	6.16	inactive	nt
PD 325901	8.46	inactive	nt
PIK-75	26.19	inactive	nt
VX-702	3.92	inactive	nt
vargatef	2.57	inactive	nt
vemurafenib	11.57	inactive	nt
ZSTK474	5.21	inactive	nt

^aNo effect up to 20 μ M concentration. ^bNot tested.

(PD-173952, PD-180970, saracatinib, and CUDC-101) were predicted to be active and one compound (tivozanib) was predicted as active or weakly active compound. The remaining 18 compounds gave positive binding free energies and were therefore predicted to be inactive.

The five compounds (PD-173952, PD-180970, CUDC-101, saracatinib, and tivozanib; Figure 6) were purchased from Selleck (Selleck, US) and tested on Myt1 using the fluorescence anisotropy based binding assay described in the Computational Methods and Experimental Section. The obtained biological activities are reported in Table 7. For two compounds (CUDC-101 and tivozanib), no binding was observed at Myt1 kinase up to 20 μ M. Therefore, these two compounds were wrongly predicted by the QM/MM-GBSA score maybe due to the selection of a wrong binding pose. For saracatinib, an IC_{50} value of 15.3 μ M ($K_i = 5.2$ μ M) was obtained which is better than that

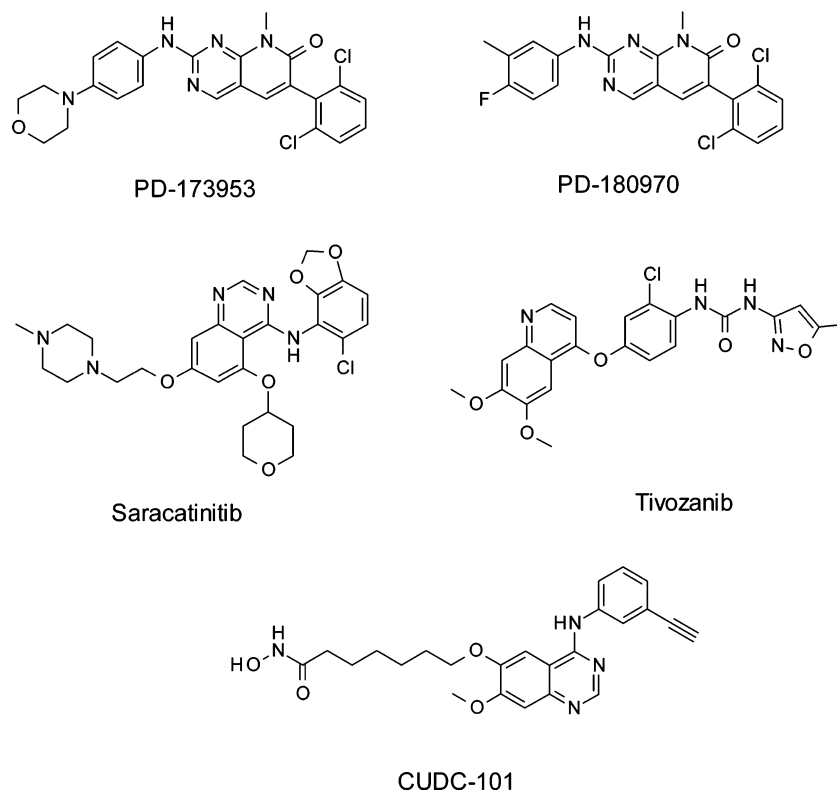


Figure 6. Chemical structures of five compounds tested for Myt1 kinase inhibition.

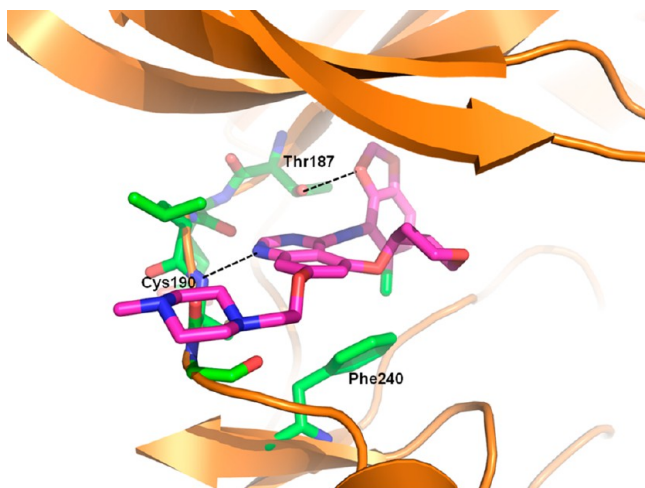


Figure 7. Predicted binding mode of saracatinib (colored magenta). The Myt1 kinase is shown as orange ribbon and green sticks. H-bond interactions are displayed as dashed lines.

of tyrphostin AG1478 ($K_i = 26 \mu\text{M}$) using the same assay.³⁴ The binding mode of saracatinib is demonstrated in Figure 7. The strongest binding was observed for PD-173952 ($K_i = 8.1 \pm 3.6 \text{ nM}$) and PD-180970 ($K_i = 1350 \pm 270 \text{ nM}$). The binding mode of the most active compound PD-173952 is displayed in Figure 8, showing that this inhibitor forms H-bond with the backbone of Cys190 at the hinge region and π - π interaction with Phe240. Interestingly, the structurally similar compound PD-180970 which also shows a favorable QM/MM-GBSA energy has a 168 fold higher K_i value. The only difference is the missing polar (morpholine) substitution at the terminal phenyl ring system. In case of PD-173952 the morpholine ring makes electrostatic interaction with Gln196 (Figure 8).

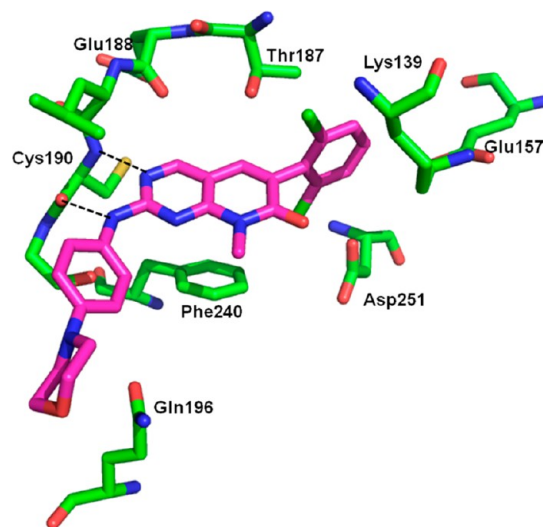


Figure 8. Predicted binding mode of the most active compound PD-173952 (colored magenta) for Myt1 kinase. Interacting amino acid residues are shown as green sticks. H-bond interactions are displayed as dashed lines.

Among all inhibitors that we have identified, we found that the compounds containing a pyridopyrimidine ring (PD-0166285, PD-173952, and PD-180970) showed the highest inhibitory activity. The complexes derived from docking and rescoring revealed that the aromatic pyrimidine ring of these compounds plays an important role for interacting with Phe240 (π - π interaction). For the inactive compounds (e.g., imatinib and bisindolyl-maleimide I) this π - π interaction was not observed. Since π - π interaction between inhibitors and Phe240 seems to play a major role for binding to Myt1, classical force fields or

docking scores lacking charge delocalization and polarization are problematic since they are not able to calculate the protein–ligand interaction correctly. Therefore, in such cases QM calculation might be a useful alternative. In our present work the QM region included Phe240, thus the π – π interaction between this residue and the inhibitors was computed by using the QM method.

4. CONCLUSION

We have successfully applied the QM/MM-GBSA rescoring method to discriminate between active and inactive Myt1 kinase inhibitors. The applied approach is fast and simple as only a single complex derived by energy minimization of the docking solutions was applied for rescoring. Time requirement of the energy minimization process is around 5–10 min per complex and for the QM/MM-GBSA calculation also approximately 5 min are required for each compound. Thus, this approach can be applied for rescoring larger data sets containing several hundreds of compounds. For selected compounds, MD simulations were also performed to compare the QM/MM-GBSA energies obtained by using a single complex and average snapshots from MD simulation. QM/MM-GBSA energies derived from MD simulation were found to correctly classify the highly active, moderately, or weakly active compounds better than using a single snapshot. Generally, the QM/MM-GBSA energies derived from both methods (energy minimization or MD simulation) can obviously discriminate between active and inactive compounds indicating that taking a single snapshot is sufficient for calculating the QM/MM-GBSA score. We have applied this approach to predict the binding energies of known kinase inhibitors from the literature. Some of these compounds which were predicted as active, weakly active or inactive compounds were selected for biological testing at Myt1 kinase. The biological data were for most of the compounds in agreement with the QM/MM-GBSA results. Only two compounds, CUDC-101 and tivozanib, were wrongly predicted to be active. Moreover, a novel potent Myt1 kinase inhibitor PD-173952 with an inhibition constant in the low nanomolar range (K_i 8.1 ± 3.6 nM) was identified using this approach. This compound represents a novel highly potent Myt1 inhibitor that will serve as a starting point for further characterization of Myt1.

Nevertheless, one has to keep in mind that the QM/MM-GBSA score is not an absolute binding free energy. In addition, there is no “gold standard” method for all systems and this approach should not be used as a “black box” to identify active binders (e.g., the QM/MM-GBSA score depends on the defined QM region and the applied QM methods). Thus, these parameters should first of all be carefully validated by using known data set and then these validated parameters can be applied further for predicting binding affinities of other compounds. In addition, the QM/MM-GBSA energies, as any scoring method, depend strongly on the quality of the docking results. Therefore the correct binding mode of each compound has to be identified, e.g. by considering crystal structures of similar compounds. Also, testing the stability of the protein–inhibitor complex derived from docking by applying MD simulations might give more confidence.

■ ASSOCIATED CONTENT

■ Supporting Information

The supporting materials include Figure S1, the binding mode of dasatinib from the X-ray structure and from docking results; Figure S2, RMSD values (Å) obtained from the MD simulations; and Figure S3, binding mode of staurosporine observed in

corresponding X-ray structures and docking poses of staurosporine and dasatinib derived from docking into Myt1 conformations taken from MD simulation runs. This material is available free of charge via the Internet at <http://pubs.acs.org>.

■ AUTHOR INFORMATION

Corresponding Author

*Phone: +49-345-55-25040. Fax: +49-345-55-27355. E-mail: wolfgang.sippl@pharmazie.uni-halle.de.

Notes

The authors declare no competing financial interest.

■ ACKNOWLEDGMENTS

The authors would like to acknowledge the European Regional Development Fund of the European Commission for financial support.

■ REFERENCES

- (1) Rapp, C.; Kalyanaraman, C.; Schiffmiller, A.; Schoenbrun, E. L.; Jacobson, M. P. A Molecular Mechanics Approach to Modeling Protein–Ligand Interactions: Relative Binding Affinities in Congeneric Series. *J. Chem. Inf. Model.* **2011**, *51*, 2082–2089.
- (2) Lindstrom, A.; Edvinsson, L.; Johansson, A.; Andersson, C. D.; Andersson, I. E.; Raubacher, F.; Linusson, A. Postprocessing of Docked Protein–Ligand Complexes Using Implicit Solvation Models. *J. Chem. Inf. Model.* **2011**, *51*, 267–282.
- (3) Wichapong, K.; Lindner, M.; Pianwanit, S.; Kokpol, S.; Sippl, W. Receptor-based 3D-QSAR studies of checkpoint Wee1 kinase inhibitors. *Eur. J. Med. Chem.* **2009**, *44*, 1383–1395.
- (4) Wichapong, K.; Lawson, M.; Pianwanit, S.; Kokpol, S.; Sippl, W. Postprocessing of Protein–Ligand Docking Poses Using Linear Response MM-PB/SA: Application to Wee1 Kinase Inhibitors. *J. Chem. Inf. Model.* **2010**, *50*, 1574–1588.
- (5) Mueller, P. R.; Coleman, T. R.; Kumagai, A.; Dunphy, W. G. Myt1 - a Membrane-Associated Inhibitory Kinase That Phosphorylates Cdc2 on Both Threonine-14 and Tyrosine-15. *Science* **1995**, *270*, 86–90.
- (6) Suganuma, M.; Kawabe, T.; Hori, H.; Funabiki, T.; Okamoto, T. Sensitization of cancer cells to DNA damage-induced cell death by specific cell cycle G2 checkpoint abrogation. *Cancer Res.* **1999**, *59*, 5887–91.
- (7) Levine, A. J. p53, the cellular gatekeeper for growth and division. *Cell* **1997**, *88*, 323–331.
- (8) Rohe, A.; Gollner, C.; Wichapong, K.; Erdmann, F.; Al-Mazaideh, G. M.; Sippl, W.; Schmidt, M. Evaluation of potential Myt1 kinase inhibitors by TR-FRET based binding assay. *Eur. J. Med. Chem.* **2013**, *61*, 41–48.
- (9) Davis, M. I.; Hunt, J. P.; Herrgard, S.; Ciceri, P.; Wodicka, L. M.; Pallares, G.; Hocker, M.; Treiber, D. K.; Zarrinkar, P. P. Comprehensive analysis of kinase inhibitor selectivity. *Nat. Biotechnol.* **2011**, *29*, 1046–1051.
- (10) Rastelli, G.; Del Rio, A.; Degliesposti, G.; Sgobba, M. Fast and Accurate Predictions of Binding Free Energies Using MM-PBSA and MM-GBSA. *J. Comput. Chem.* **2010**, *31*, 797–810.
- (11) Hou, T.; Wang, J.; Li, Y.; Wang, W. Assessing the performance of the MM/PBSA and MM/GBSA methods. I. The accuracy of binding free energy calculations based on molecular dynamics simulations. *J. Chem. Inf. Model.* **2011**, *51*, 69–82.
- (12) Kuhn, B.; Gerber, P.; Schulz-Gasch, T.; Stahl, M. Validation and use of the MM-PBSA approach for drug discovery. *J. Med. Chem.* **2005**, *48*, 4040–4048.
- (13) Hou, T.; Wang, J.; Li, Y.; Wang, W. Assessing the performance of the molecular mechanics/Poisson Boltzmann surface area and molecular mechanics/generalized Born surface area methods. II. The accuracy of ranking poses generated from docking. *J. Comput. Chem.* **2011**, *32*, 866–877.
- (14) Weis, A.; Katebzadeh, K.; Soderhjelm, P.; Nilsson, I.; Ryde, U. Ligand affinities predicted with the MM/PBSA method: Dependence

on the simulation method and the force field. *J. Med. Chem.* **2006**, *49*, 6596–6606.

(15) *Molecular Operating Environment (MOE)*; 2011.10, Chemical Computing Group, Inc.: Montreal, Canada. 2011.

(16) Jones, G.; Willett, P.; Glen, R. C. Molecular recognition of receptor sites using a genetic algorithm with a description of desolvation. *J. Mol. Biol.* **1995**, *245*, 43–53.

(17) Jones, G.; Willett, P.; Glen, R. C.; Leach, A. R.; Taylor, R. Development and validation of a genetic algorithm for flexible docking. *J. Mol. Biol.* **1997**, *267*, 727–748.

(18) Kolb, P.; Huang, D.; Dey, F.; Caflisch, A. Discovery of kinase inhibitors by high-throughput docking and scoring based on a transferable linear interaction energy model. *J. Med. Chem.* **2008**, *51*, 1179–1188.

(19) Lyne, P. D.; Lamb, M. L.; Saeh, J. C. Accurate prediction of the relative potencies of members of a series of kinase inhibitors using molecular docking and MM-GBSA scoring. *J. Med. Chem.* **2006**, *49*, 4805–4808.

(20) Case, D. A.; Darden, T. A.; Cheatham, I. T. E.; Simmerling, C. L.; Wang, J.; Duke, R. E.; Luo, R.; Crowley, M.; Walker, R. C.; Zhang, W.; Merz, K. M.; Wang, B.; Hayik, S.; Roitberg, A.; Seabra, G.; Kolossváry, I.; Wong, K. F.; Paesani, F.; Vanicek, J.; Wu, X.; Brozell, S. R.; Steinbrecher, T.; Gohlke, H.; Yang, L.; Tan, C.; Mongan, J.; Hornak, V.; Cui, G.; Mathews, D. H.; Seetin, M. G.; Sagui, C.; Babin, V.; Kollman, P. A. *AMBER 11*; University of California, San Francisco, 2010.

(21) Wang, J. M.; Wolf, R. M.; Caldwell, J. W.; Kollman, P. A.; Case, D. A. Development and testing of a general amber force field. *J. Comput. Chem.* **2004**, *25*, 1157–1174.

(22) Jakalian, A.; Jack, D. B.; Bayly, C. I. Fast, efficient generation of high-quality atomic charges. AM1-BCC model: II. Parameterization and validation. *J. Comput. Chem.* **2002**, *23*, 1623–1641.

(23) Still, W. C.; Tempczyk, A.; Hawley, R. C.; Hendrickson, T. Semianalytical Treatment of Solvation for Molecular Mechanics and Dynamics. *J. Am. Chem. Soc.* **1990**, *112*, 6127–6129.

(24) Srinivasan, J.; Trevathan, M. W.; Beroza, P.; Case, D. A. Application of a pairwise generalized Born model to proteins and nucleic acids: inclusion of salt effects. *Theor. Chem. Acc.* **1999**, *101*, 426–434.

(25) Luo, R.; David, L.; Gilson, M. K. Accelerated Poisson-Boltzmann calculations for static and dynamic systems. *J. Comput. Chem.* **2002**, *23*, 1244–1253.

(26) Hayik, S. A.; Dunbrack, R., Jr.; Merz, K. M., Jr. A Mixed QM/MM Scoring Function to Predict Protein-Ligand Binding Affinity. *J. Chem. Theory Comput.* **2010**, *6*, 3079–3091.

(27) Raha, K.; Merz, K. M., Jr. A quantum mechanics-based scoring function: study of zinc ion-mediated ligand binding. *J. Am. Chem. Soc.* **2004**, *126*, 1020–1021.

(28) Thompson, D. C.; Humblet, C.; Joseph-McCarthy, D. Investigation of MM-PBSA rescoring of docking poses. *J. Chem. Inf. Model.* **2008**, *48*, 1081–1091.

(29) Jorgensen, W. L.; Chandrasekhar, J.; Madura, J. D.; Impey, R. W.; Klein, M. L. Comparison of simple potential functions for simulating liquid water. *J. Chem. Phys.* **1983**, *79*, 926–935.

(30) Pastor, R. W.; Brooks, B. R.; Szabo, A. An Analysis of the Accuracy of Langevin and Molecular-Dynamics Algorithms. *Mol. Phys.* **1988**, *65*, 1409–1419.

(31) Ryckaert, J.-P.; Ciccotti, G.; Berendsen, H. J. C. Numerical integration of the cartesian equations of motion of a system with constraints: molecular dynamics of n-alkanes. *J. Comput. Phys.* **1977**, *23*, 327–341.

(32) Darden, T.; York, D.; Pedersen, L. Particle mesh Ewald: An Nlog(N) method for Ewald sums in large systems. *J. Chem. Phys.* **1993**, *98*, 10089–10092.

(33) Rohe, A.; Erdmann, F.; Bassler, C.; Wichapong, K.; Sippl, W.; Schmidt, M. In vitro and in silico studies on substrate recognition and acceptance of human PKMYT1, a Cdk1 inhibitory kinase. *Bioorg. Med. Chem. Lett.* **2012**, *22*, 1219–1223.

(34) Rohe, A.; Henze, C.; Erdmann, F.; Sippl, W.; Schmidt, M. A Fluorescence Anisotropy-Based Myt1 Kinase Binding Assay. *Assay Drug Dev. Technol.* **2013**, DOI: 10.1089/adt.2013.534.